SUPPLEMENTARY INFORMATION

Structure and mechanism of an Fe(II)/α-ketoglutarate-dependent sulfoquinovose diooxygenase

Mihwa Lee [a]*, Ho N. N. Ho[a], Megan J. Maher [a], Guy N.L. Jameson,[a]* Spencer J. Williams [a]*

[a] School of Chemistry and Bio21 Molecular Science and Biotechnology Institute, University of Melbourne, Parkville, Victoria 3010, Australia

SUPPLEMENTARY INFORMATION

Cloning, protein expression and purification of *Marinobacterium aestuarii* SqoD

The codon-optimized DNA sequence encoding *Ma*SqoD (WP_067381946.1), featuring an N-terminal hexa-histidine (His_6) tag followed by a TEV protease recognition site, was synthesized and cloned into pET28a between the *NcoI* and *XhoI* restriction sites. For protein production, pET28a-*Ma*SqoD was transformed into *E. coli* BL21(DE3). The cells were grown in lysogeny broth containing 50 μg/ml kanamycin at 37 °C and induced with 0.4 mM isopropyl 1-thio-β-D-galactopyranoside (IPTG) upon reaching an A_{600} of 0.8. After incubation at 18 °C for 16 h, cells were harvested by centrifugation at 6000 × *g*. The pellet was resuspended in buffer A (20 mM Tris · HCl, pH 7.5, 500 mM NaCl, 25 mM imidazole), lysed using a TS Series benchtop cell disruptor, and clarified by centrifugation at 35000 × *g*. The soluble fraction was applied to a Ni^{2+}-charged chelating column (Hi-Trap HP, Cytiva) and eluted using a 25–500 mM imidazole gradient in buffer A. Pooled fractions were treated with tobacco etch virus (TEV) protease at a 1:20 (w:w) ratio in dialysis tubing (10 kDa MWCO) and dialyzed against buffer B (20 mM Tris · HCl, pH 7.5, 200 mM NaCl) for 2 h at room temperature. To separate uncleaved protein and His_6-tagged TEV protease, the dialyzed sample was applied to a Ni^{2+}-charged Hi-Trap column, and unbound fractions were collected. Further purification was performed using size-exclusion chromatography with a HiLoad 16/600 Superdex 200 pg column equilibrated with buffer B. Final protein samples, for enzyme assays and crystallisation, were concentrated to 5–15 mg/ml, snap-frozen using liquid nitrogen and stored at − 80 °C. For stopped-flow spectroscopy, protein samples were treated with 1 mM EDTA before the size-exclusion chromatography step to remove any residual metals (such as Ni^{2+} from the IMAC purification step) and the final samples were concentrated to 48–70 mg/ml.

Enzyme kinetics

Fuchsin assays

*Ma*SqoD activity was measured using a stopped assay by quantifying sulfite using a modified version of the previously reported colorimetric Fuchsin assay method.[1] Briefly, 25 μl of the reaction sample and 5 μl of 0.4 mM sodium sulfite were added to 170 μl of freshly prepared Fuchsin reagent (0.04% Fuchsin in 25% sulfuric acid mixed with 1.08% formaldehyde and deionized water at 1:1:7 ratio). After 10 min incubation at room temperature for colour development, the absorbance at 570 nm was measured using a 96-well plate reader to detect the coloured sulfite-Fuchsin complex, and sulfite concentration was calculated using a standard curve generated with 0–0.5 mM sulfite, which was established for each reaction condition and included metal salt and substrates.

Kinetic data analysis

Data analysis and calculation of the apparent kinetic parameters, k_{cat}^{app}, K_M^{app} and $(k_{cat}/K_M)^{app}$ were performed using Prism 10 (GraphPad Scientific Software). All measurements were performed in triplicate, and error bars represent standard deviation. Kinetic data for αKG were fit to the substrate

inhibition kinetic equation (1) where [S] is the concentration of substrate, V_{max} is the limiting reaction rate (mM s^{-1}), v is the initial reaction rate (mM s^{-1}).

$$v = \frac{V_{max}[S]}{K_M' + [S] + \frac{[S]^2}{K_I}} \quad (1)$$

pH dependence of MaSqoD

Enzyme reaction mixtures (0.4 ml final volume) containing 5 mM SQ, 5 mM α-KG, 0.25 mM $FeCl_2$, 0.5 mM sodium L-ascorbate, and 1.9 μM *Ma*SqoD were prepared in 80 mM buffer within the range pH 6.0–9.0 (Bis-Tris HCl, pH 6.0; Tris-HCl, pH 7.0, 7.5, 8.0 and 9.0) containing 100 mM NaCl, and 0.1% bovine serum albumin (BSA). The reactions were incubated at 30 ºC for 4 min, then quenched by direct addition into the Fuchsin solution and assayed as described above.

Metal dependence of MaSqoD

Enzyme reaction mixtures (0.4 ml final volume) containing 5 mM SQ, 5 mM α-KG, 0.25 mM MCl_2 or MSO_4 ($FeCl_2$, $MnCl_2$, $CoCl_2$, $NiSO_4$, or $ZnCl_2$), 0.5 mM sodium L-ascorbate, and 1.9 μM *Ma*SqoD were prepared in 80 mM Tris-HCl (pH 7.5) containing 100 mM NaCl, and 0.1% BSA. The reactions were incubated at 30 ºC for 30 min, then quenched by direct addition into the Fuchsin solution and assayed as described above.

Michaelis Menten kinetic analysis of MaSqoD

Michaelis Menten kinetic analysis of *Ma*SqoD was performed under pseudo-first-order conditions, where the concentration of one substrate (SQ or αKG) was held constant at 5 mM, while the other was varied: [SQ] from 0.5–30 mM and [αKG] from 0.05–15 mM. Reactions (0.4 ml) were conducted at 30 ºC in 80 mM Tris-HCl (pH 7.5) containing 100 mM NaCl, 0.1% BSA, 0.25 mM $FeCl_2$, and 0.5 mM sodium L-ascorbate. Reaction rates were measured over 6 min following addition of *Ma*SqoD (1.9 μM final concentration): 25 μl of the reaction sample was taken at 0, 2, 4, and 6 min, and quenched by direct addition into the Fuchsin solution and assayed as described above.

Stopped-flow kinetics

Stopped-flow measurements were performed on a SX-20MV stopped-flow spectrometer equipped with a Xe arc lamp (Applied Photophysics). Prior to measurements, Fe(II) was loaded to *Ma*SqoD by mixing with equimolar ammonium iron(II) sulfate hexahydrate and a small excess of sodium dithionite (~1:1:1.1). The apparatus was then used to rapidly mix an anaerobically prepared *Ma*SqoD•Fe(II)•αKG•SQ complex (~1:5:5 equivalents, [*Ma*SqoD] ~1 mM) with oxygenated buffer (1:1 v/v) at 4.5 °C, yielding an estimated [O_2] of ~2 mM. Temperature was maintained using a refrigerated, closed-circuit water bath (DC10-K10, Haake).

SUPPLEMENTARY INFORMATION

Before each experiment, the drive syringes and flow circuit were flushed with 3 mM sodium dithionite solution and extensively rinsed with deoxygenated buffer. Kinetic experiments were conducted in single-mixing mode and monitored using either a photodiode array or photomultiplier detector. Single-wavelength traces (310–800 nm) were analyzed using SX20 Pro-Data Viewer software (Applied Photophysics). Spectral changes in the 300–723 nm range were further examined by global analysis with PC Pro-K software (Applied Photophysics). Data were subsequently processed and plotted using Excel (Microsoft) and Prism 11 (GraphPad).

Protein crystallization and ligand soaking

Crystals of *Ma*SqoD were grown by hanging-drop vapor diffusion at 20 °C. A 2 µl aliquot of protein (8.2 mg/ml) was mixed with an equal volume of reservoir solution (1.8–2.1 M sodium malonate, pH 5.5–6.0) and equilibrated against 0.5 ml of the reservoir solution. Prior to ligand soaking experiments, crystals were transferred to hanging drops containing 2.2 M ammonium sulfate, 50 mM MES, pH 5.5–6.0 and incubated at least 1 day. *Ma*SqoD•SQ complexes were obtained by transferring these pre-incubated crystals to drops containing 50 mM SQ, 2.2 M ammonium sulfate, 50 mM MES pH 5.5–6.0 for 2 days.

Crystals of *Ma*SqoD in complex with cofactor (αKG or succinate) and Mn^{2+} were obtained by sequential transfers of crystals: first to a Mn^{2+}-containing solution (2 mM $MnCl_2$, 2.2 M ammonium sulfate, 50 mM MES, pH 5.5–6.0) for 1–2 days, followed by transfer to a solution containing both Mn^{2+} and cofactor (2 mM $MnCl_2$, 10 mM αKG or sodium succinate, 2.2 M ammonium sulfate, 50 mM MES, pH 5.5–6.0) for an additional 1–2 days prior to harvesting.

Crystals of *Ma*SqoD in complex with αKG, Mn^{2+}, and SQ were obtained by transferring crystals pre-soaked in a solution containing αKG and Mn^{2+} to a final soaking solution containing 50 mM SQ, 2 mM $MnCl_2$, 10 mM αKG, 2.2 M ammonium sulfate, and 50 mM MES (pH 5.5–6.0) for 1–2 days prior to harvest.

X-ray diffraction data collection, crystal structure determination and refinement

Crystals were cryocooled in liquid nitrogen without additional cryoprotection. Diffraction data were collected at 100 K on beamline MX2 at the Australian Synchrotron[2] using a wavelength of 0.954 Å. The data were processed with XDS[3] and merged and scaled using AIMLESS.[4] Data collection and merging statistics are summarized in **Table S1**.

The crystal structure of malonate-bound *Ma*SqoD was solved by molecular replacement using PHASER[5] within the CCP4 suite.[6] The AlphaFold2[7] predicted model of *Ma*SqoD (AF-A0A1A9EZ58-F1) was used as the initial search model, yielding a solution with a log-likelihood gain of 171 and a Z-score of 15.0, locating a monomer in the asymmetric unit. Significant rebuilding of residues 169–227 was required due to domain closure (**Figure S2**). Iterative model building and refinement were

performed using COOT[8] and REFMAC,[9] respectively. For the structures of complexes, the malonate-bound *Ma*SqoD coordinates were used as the initial refinement model after removing all non-protein atoms and setting the temperature factor to 30 Å^2. Model quality was validated using MOLPROBITY.[10] Refinement statistics are included in **Table S1**.

SUPPLEMENTARY INFORMATION

Table S1. Diffraction data and refinement statistics.[a]

Data collection	Malonate-bound	*Ma*SqoD•SQ	*Ma*SqoD•Mn^{2+}•αKG	*Ma*SqoD•Mn^{2+}•αKG•SQ	*Ma*SqoD•Mn^{2+}•succinate
Space group	$C222_1$	$C222_1$	$C222_1$	$C222_1$	$C222_1$
Unit cell parameters (Å)	109.0, 117.1, 59.3	107.7, 118.3, 59.1	108.7, 117.7, 59.4	108.9, 118.0, 59.5	108.6, 117.7, 59.1
Resolution (Å)	47.61–1.42 (1.4 –1.42)	47.43–1.45 (1.47–1.45)	47.64–2.04 (2.09–2.04)	47.75–2.10 (2.16 – 2.10)	47.48–1.57 (1.60–1.57)
No. of observations	479,222 (21,321)	452,290 (21,324)	165,379 (115.57)	154,972 (12,611)	343,208 (15,106)
No. of unique reflections	71,275 (3,261)	66,993 (3,200)	24,768 (1,736)	22,708 (1,798)	52,605 (2,440)
Completeness (%)	99.7 (93.3)	99.9 (97.5)	99.8 (97.3)	99.7 (97.9)	99.5 (93.9)
Redundancy	6.7 (6.5)	6.8 (6.7)	6.7 (6.7)	6.8 (7.0)	6.5 (6.2)
R_{merge} (%)	5.7 (80.0)	4.4 (59.9)	7.3 (99.3)	5.8 (70.0)	8.8 (54.5)
R_{pim} (%)	2.6 (37.0)	2.0 (28.6)	3.3 (44.9)	2.6 (30.6)	4.2 (25.8)
$CC_{1/2}$	1.00 (0.77)	1.00 (0.81)	1.00 (0.61)	1.00 (0.79)	1.00 (0.84)
Average $I/\sigma(I)$	12.3 (1.5)	15.0 (2.0)	11.2 (1.2)	13.3 (1.8)	11.1 (2.2)
Refinement					
R (%)	12.5 (22.6)	12.6 (19.7)	19.1 (29.1)	19.3 (26.6)	16.6 (23.1)
R_{free} (%)	15.7 (24.9)	16.0 (21.8)	22.8 (34.1)	22.6 (30.4)	18.9 (26.0)
No. (%) of reflections in test set	3,599 (5.1)	3,379 (5.0)	1,303 (5.3)	1,130 (5.0)	2,604 (5.0)
No. of protein molecules per asu	1	1	1	1	1
R.m.s.d. bond length (Å)	0.007	0.007	0.005	0.005	0.006
R.m.s.d. bond angle (°)	1.556	1.593	1.374	1.355	1.473
Average B-factors ($Å^2$)[b]	20.3	22.2	43.2	43.6	18.5
Protein molecules	18.3	19.9	43.2	43.7	16.7

Ligands					
substrate (SQ)	-	17.9	-	54.9*	-
cofactor	-	-	43.0*	46.3*	16.3
Mn^{2+}	-	-	36.0*	48.2*	13.4
malonate	16.8 (αKG site) 22.0 (SQ site)	-	-	-	-
Water molecules	32.9	35.7	41.5	43.3	28.4
Ramachandran plot[c]					
Residues other than Gly and Pro in:					
Most favoured regions (%)	98.8	98.9	98.1	98.1	98.8
Additionally allowed regions (%)	1.2	1.1	1.9	1.9	1.2
Outliers (%)	0.0	0.0	0.0	0.0	0.0
PDB entry code	9YUT	9YUU	9YUV	9YUW	9YUX

* Final coordinates modelled with the occupancy of 0.8.

SUPPLEMENTARY INFORMATION

Supplementary Figures

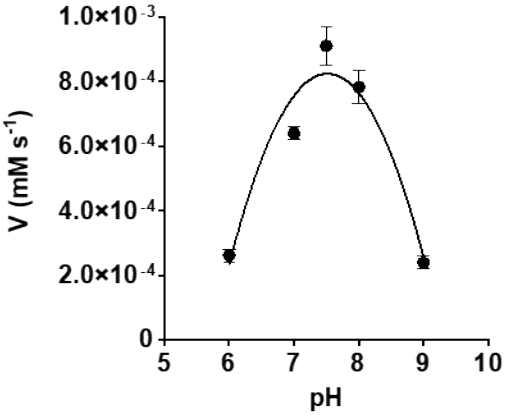

Figure S1. pH dependence of reaction rate for *Ma*SqoD. Enzyme activity was measured across varying pH conditions in 80 mM buffer within the range pH 6.0–8.0 (Bis-Tris HCl, pH 6.0; Tris-HCl, pH 7.0, 7.5, 8.0 and 9.0) with 100 mM NaCl, 0.1% BSA, 5 mM SQ, 5 mM α-KG, 0.25 mM $FeCl_2$, and 0.5 mM sodium L-ascorbate. Reactions were initiated by the addition of *Ma*SqoD to a final concentration of 1.9 μM. Sulfite production was quantified using a colorimetric Fuschsin assay.

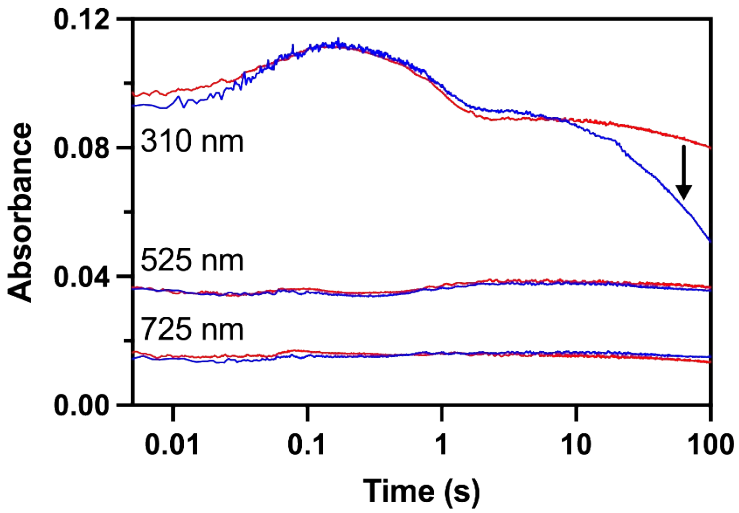

Figure S2. Effect of photolysis over longer time periods. The kinetic profiles at three wavelengths (310, 525 and 725 nm) determined using white light and a PDA (blue) and a monochromator (1 mm slit width) (red). Major differences between the two methods of detection only occur at times >10s and at lower wavelength (310 nm). The difference related to light intensity can be explained by photolysis of most likely a ferric species after a single turnover has completed.

SUPPLEMENTARY INFORMATION

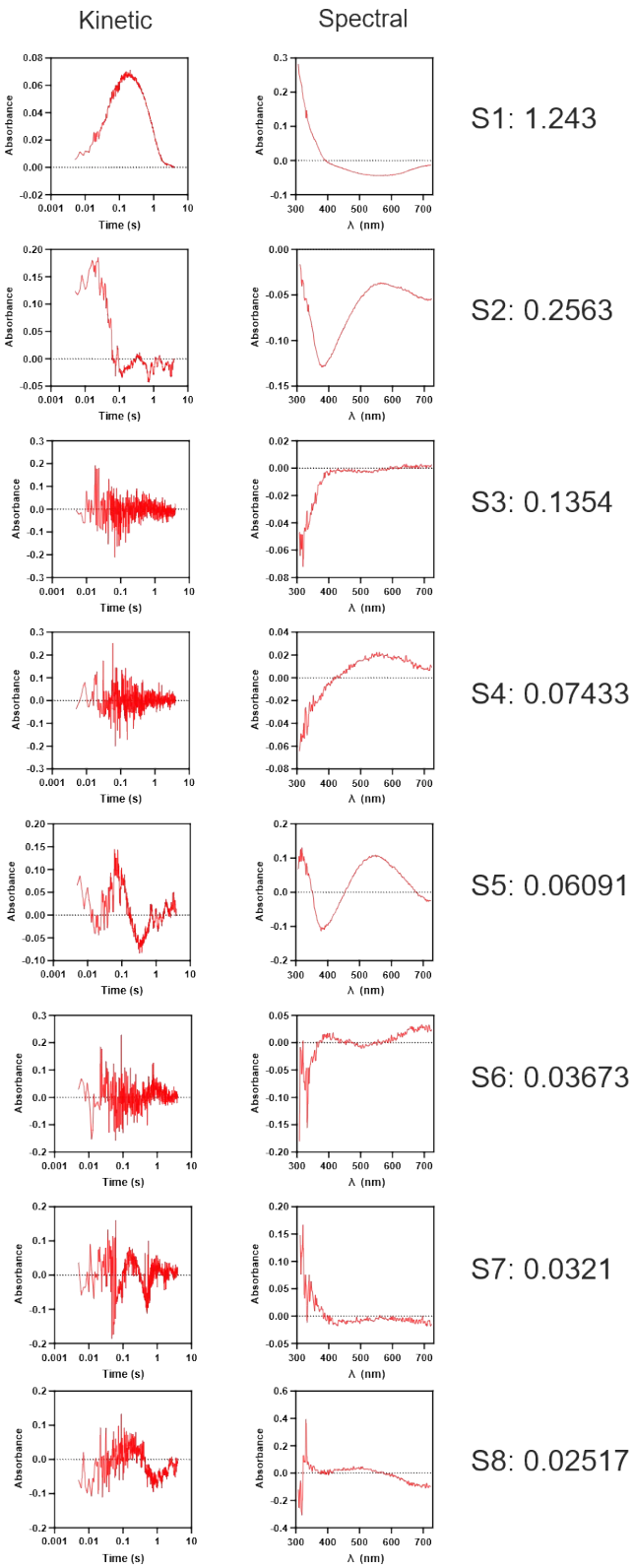

Figure S3. Identification of reaction intermediates by stopped-flow spectroscopy. Single value decomposition of the stopped-flow absorption spectra identified five discrete kinetic and spectral components, suggesting the formation of multiple reaction intermediates during turnover of the *Ma*SqoD•αKG•SQ complex with O_2.

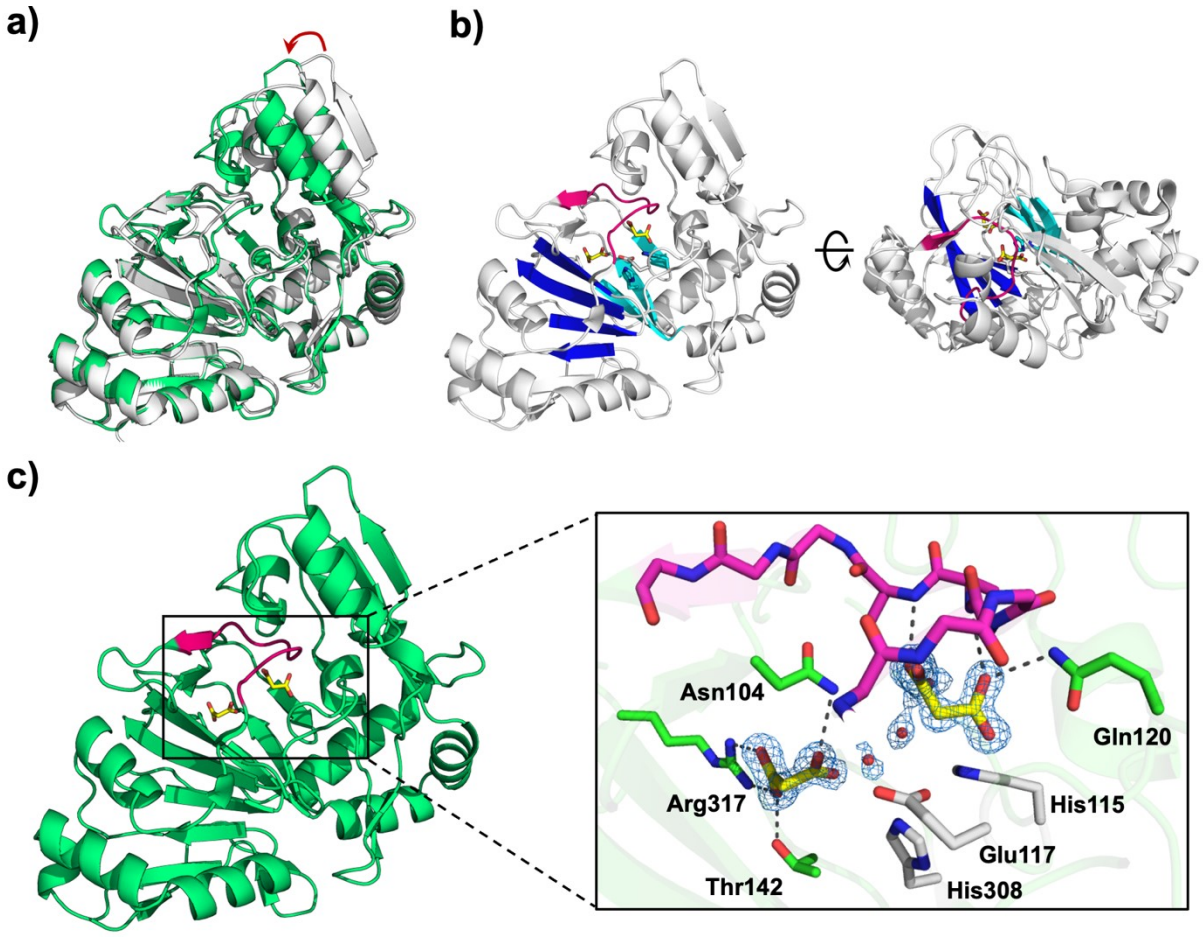

Figure S4. Comparison of the crystal structure of malonate-bound *Ma*SqoD and the AlphaFold2 model. a) Superposition of malonate-bound *Ma*SqoD structure (green) with the AlphaFold2 model (light grey; AF-A0A1A9EZ58-F1). The red arrow highlights the domain closure in the malonate-bound crystal structure of *Ma*SqoD, leading to a more compact structure. **b**) Jelly-roll topology of *Ma*SqoD. β-strands in the barrel are coloured in blue and cyan. The bound malonate molecules (carbon atoms in yellow) and predicted metal-coordinating triad (His115, Glu117, and His308) are shown to indicate the active-site location within the barrel. The active-site flexible loop (residues 84–93) is highlighted in magenta. **c**) The overall structure of *Ma*SqoD•(malonate)$_2$ complexis shown on the left panel with the active-site flexible loop (residues 84–93) highlighted in magenta and the ligands bound in the active site shown in stick representation The main chain of the flexible loop in the zoomed-in panel is shown in stick representation (carbon atoms in magenta). Carbon atoms of metal-coordinating triad (His115, Glu117, and His308) are shown in light grey. Electron density maps shown in blue mesh are $2F_o - F_c$ maps contoured at 1 σ.

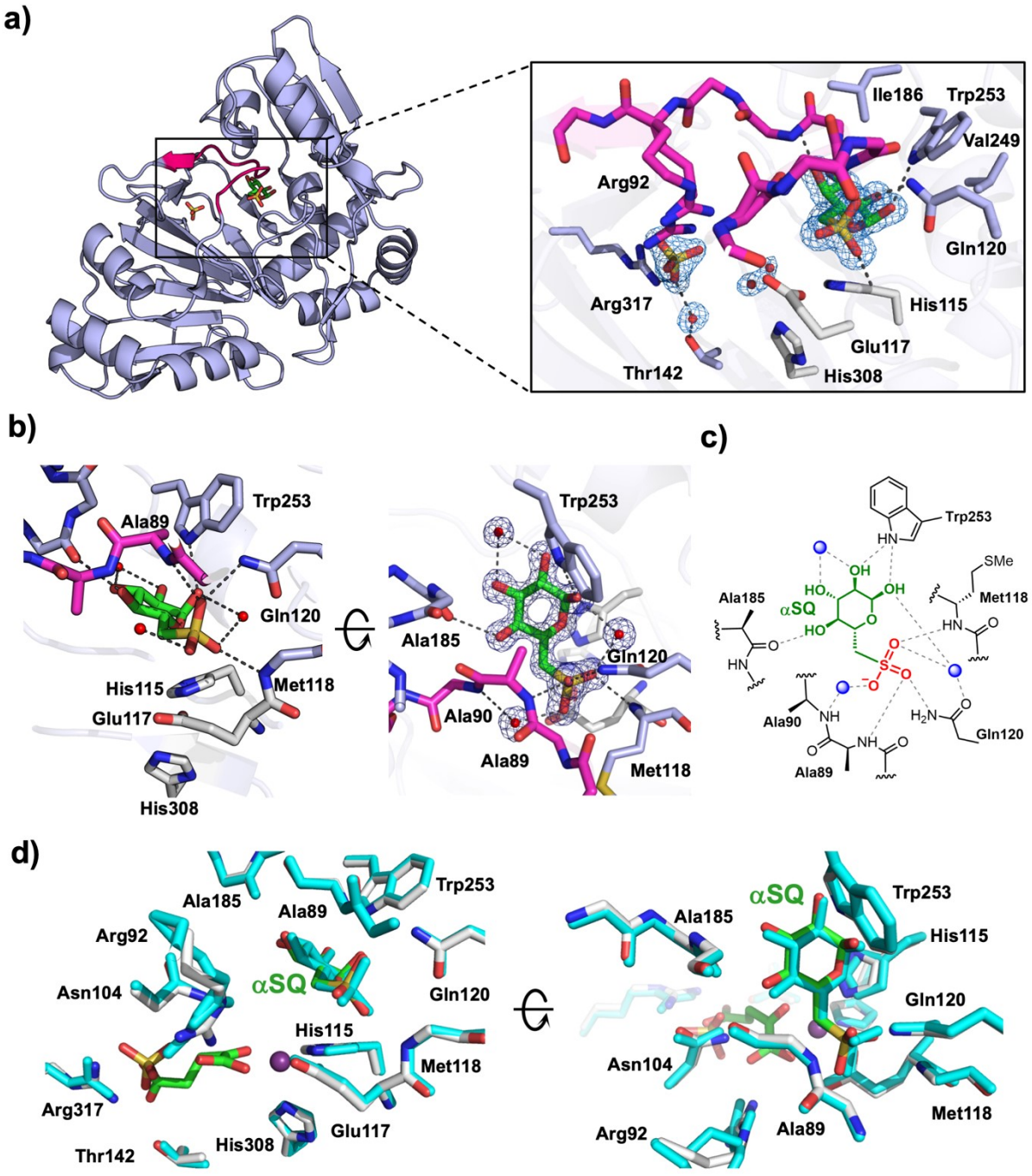

Figure S5. 3D crystal structure of *Ma*SqoD in complex with SQ. a) Overall structure of *Ma*SqoD in complex with SQ. The active-site flexible loop (residues 84–93) is highlighted in magenta and the ligands bound in the active site are shown in stick representation. Carbon atoms of metal-coordinating triad (His115, Glu117, and His308) are shown in light grey. Electron density maps shown in blue mesh are 2*F*o – *F*c maps contoured at 1 σ. The main chain of the flexible loop in the zoomed-in panel is shown in stick representation (carbon atoms in magenta). **b**) SQ-binding mode in the *Ma*SqoD•SQ complex. **c**) An illustration highlighting key interactions from b). Blue spheres represent water molecules and dotted lines hydrogen bonds. **d**) Comparison of the active sites of the *Ma*SqoD•Mn^{2+}•αKG•SQ and *Ma*SqoD•SQ complexes. The colour scheme of the

SUPPLEMENTARY INFORMATION

*Ma*SqoD•Mn^{2+}•αKG•SQ complex is same as shown in **Figure 4b** while all atoms in the *Ma*SqoD•SQ complex are shown in cyan except for the sulfate molecule bound to Arg317 (oxygen in red and sulfur in gold).

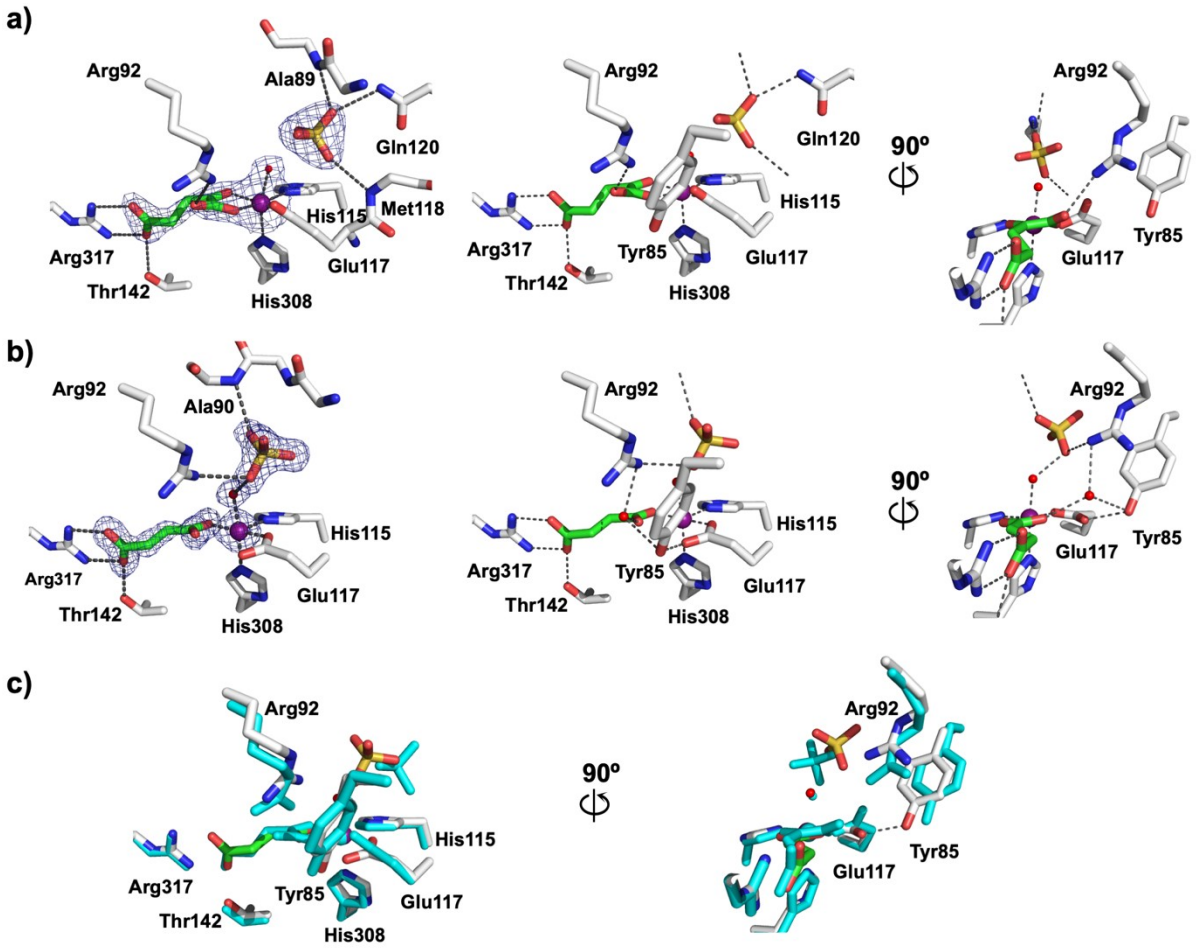

Figure S6. Active-site comparison of αKG-bound and succinate-bound *Ma*SqoD complexes. a) *a*KG-bound *Ma*SqoD complex, **b**) succinate-bound *Ma*SqoD complex, and **c**) superposition of the two structures with αKG-bound complex in cyan and the succinate-bound complex shown as in panel **b**. Hydrogen-bond interaction between Glu117 and Tyr85 in the succinate-bound complex is shown in the right panel. Electron density maps shown in blue mesh are 2*F*o – *F*c maps contoured at 1 σ.

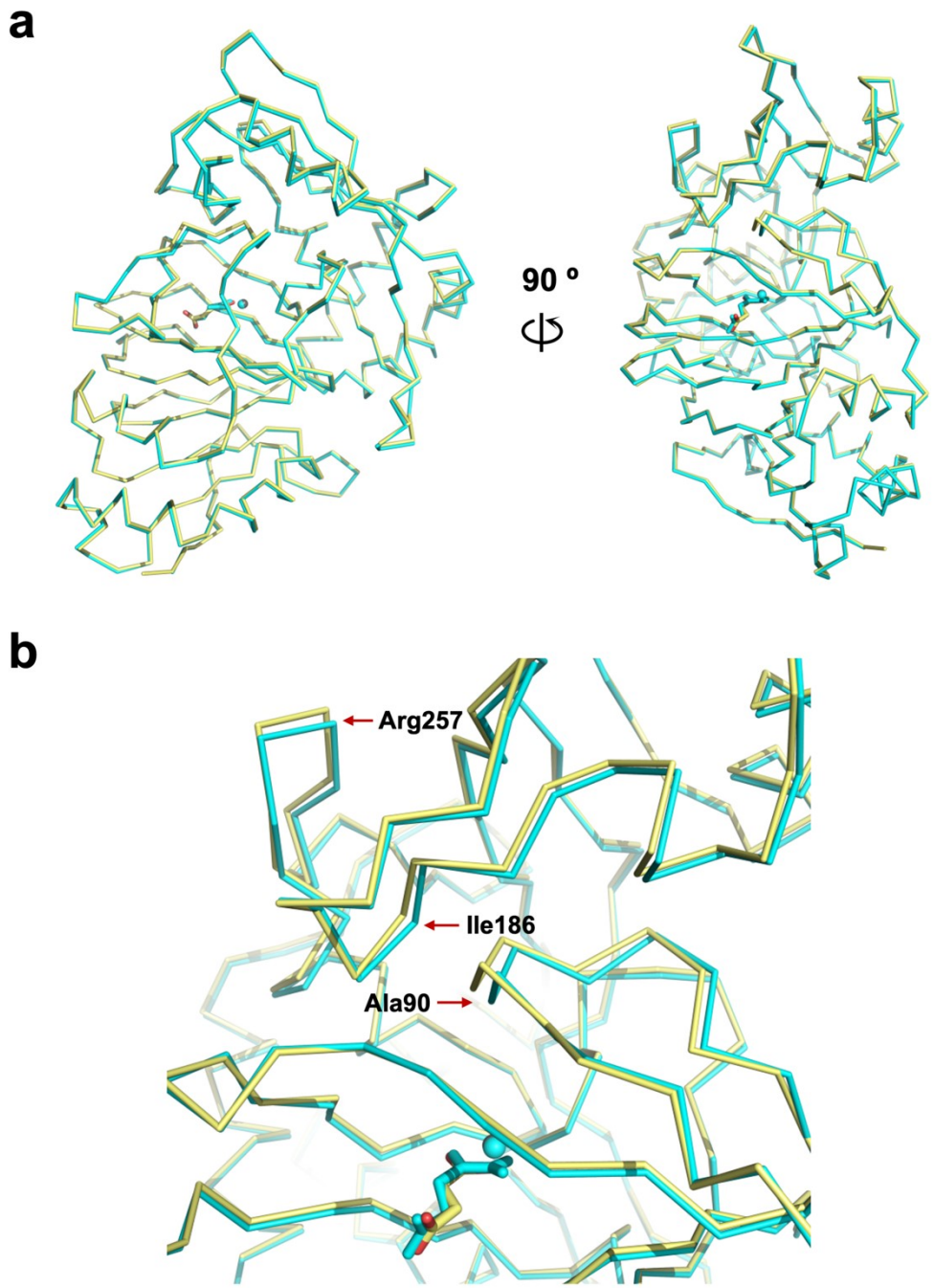

Figure S7. Overall conformation comparison of αKG-bound and succinate-bound *Ma*SqoD complexes. a) Superposition of αKG-bound complex (cyan) with succinate-bound complex (yellow). b) Zoomed-in view of loop conformations near the active site including the active-site loop (residues 84 – 93) and adjacent loops, highlighting the more open conformation when succinate is bound in the active site.

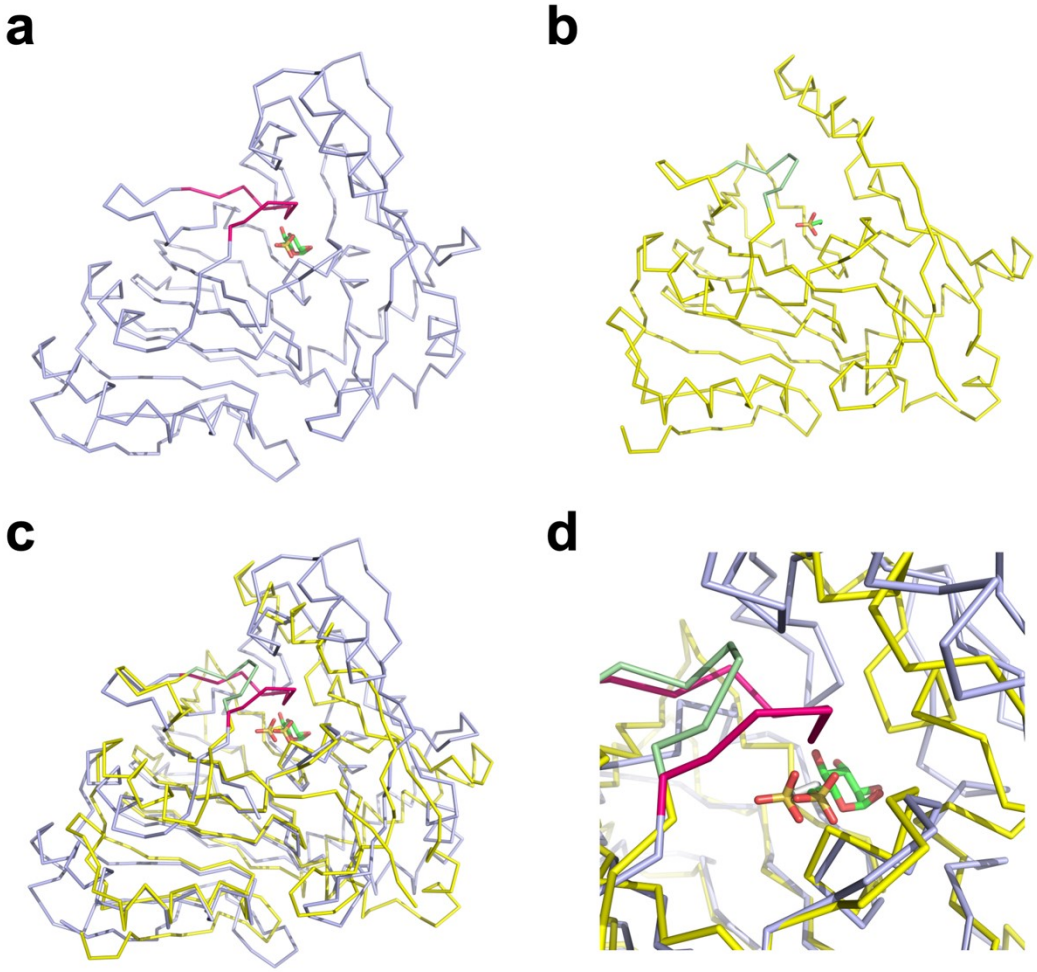

Figure S8. Comparison of substrate-binding modes in *Ma*SqoD and *Ec*TauD. a) *Ma*SqoD, **b**) *Ec*TauD (PDB entry 1OTJ), **c**) the overall superposition of the two enzyme structures, and **d**) the zoomed active sites. The active-site loop of *Ma*SqoD is coloured in magenta while the equivalent loop in *Ec*TauD in green. While the approximate position of sulfonate group is similar relative to the metal centre, residues coordinating sulfonate group are different in the two enzymes. To facilitate the binding of a sugar ring, an additional domain above the active site loop is involved in coordinating SQ in *Ma*SqoD.

SUPPLEMENTARY INFORMATION

Supplementary References

(1) Kurmanbayeva, A.; Brychkova, G.; Bekturova, A.; Khozin, I.; Standing, D.; Yarmolinsky, D.; Sagi, M. Determination of Total Sulfur, Sulfate, Sulfite, Thiosulfate, and Sulfolipids in Plants. In *Plant Stress Tolerance: Methods and Protocols*, Sunkar, R. Ed.; Springer New York, 2017; pp 253-271.
(2) Aragao, D.; Aishima, J.; Cherukuvada, H.; Clarken, R.; Clift, M.; Cowieson, N. P.; Ericsson, D. J.; Gee, C. L.; Macedo, S.; Mudie, N.; et al. MX2: a high-flux undulator microfocus beamline serving both the chemical and macromolecular crystallography communities at the Australian Synchrotron. *J. Synchrotron Radiation* **2018**, *25*, 885-891.
(3) Kabsch, W. Xds. *Acta Crystallogr., Section D: Biol. Crystallogr.* **2010**, *66*, 125-132.
(4) Evans, P. R.; Murshudov, G. N. How good are my data and what is the resolution? *Acta Crystallogr. Sect. D* **2013**, *69*, 1204-1214.
(5) McCoy, A. J.; Grosse-Kunstleve, R. W.; Adams, P. D.; Winn, M. D.; Storoni, L. C.; Read, R. J. Phaser crystallographic software. *J. Appl. Crystallogr.* **2007**, *40*, 658-674.
(6) Winn, M. D.; Ballard, C. C.; Cowtan, K. D.; Dodson, E. J.; Emsley, P.; Evans, P. R.; Keegan, R. M.; Krissinel, E. B.; Leslie, A. G. W.; McCoy, A.; et al. Overview of the CCP4 suite and current developments. *Acta Crystallogr. D* **2011**, *67*, 235-242.
(7) Jumper, J.; Evans, R.; Pritzel, A.; Green, T.; Figurnov, M.; Ronneberger, O.; Tunyasuvunakool, K.; Bates, R.; Žídek, A.; Potapenko, A.; et al. Highly accurate protein structure prediction with AlphaFold. *Nature* **2021**, *596*, 583-589.
(8) Emsley, P.; Lohkamp, B.; Scott, W. G.; Cowtan, K. Features and development of Coot. *Acta Crystallogr. Sect. D* **2010**, *66*, 486-501.
(9) Winn, M. D.; Murshudov, G. N.; Papiz, M. Z. Macromolecular TLS refinement in REFMAC at moderate resolutions. *Methods Enzymol.* **2003**, *374*, 300-321.
(10) Williams, C. J.; Headd, J. J.; Moriarty, N. W.; Prisant, M. G.; Videau, L. L.; Deis, L. N.; Verma, V.; Keedy, D. A.; Hintze, B. J.; Chen, V. B.; et al. MolProbity: More and better reference data for improved all-atom structure validation. *Protein Sci.* **2018**, *27*, 293-315.